

Optimal Cruise, Descent, and Landing of eVTOL Vehicles for Urban Air Mobility using Convex Optimization

Zhenbo Wang*

University of Tennessee, Knoxville, Tennessee 37996, USA

Peng Wei†

George Washington University, Washington, DC 20052, USA

Liang Sun‡

New Mexico State University, Las Cruces, New Mexico 88003, USA

In this paper, we propose a novel approach to trajectory optimization of electric vertical takeoff and landing (eVTOL) vehicles for urban air mobility (UAM) missions such as passenger transportation and cargo delivery. Our particular interest is to develop efficient algorithms that facilitate fast generation of optimal cruise, descent, and landing trajectories for eVTOL vehicles under operational constraints. As a preliminary study, we focus on the formulation of an optimal control problem with fixed time of flight and choose the control effort as the performance measure for a multirotor eVTOL vehicle. The main contribution of this work is the convexification of the formulated optimal control problem to better enable real-time trajectory optimization with required time of arrival, which is of key importance for future eVTOL operations. The convexification process is presented in this paper. The EHang 184 eVTOL vehicle is used in the simulations, and preliminary results of a UAM transportation case are provided to demonstrate the effectiveness of the proposed approach.

Nomenclature

C_D	=	drag coefficient
D	=	drag force, N
g	=	gravitational acceleration, m/s ²
m	=	vehicle's mass, kg
S_x	=	reference front plate area, m ²
S_z	=	reference top plate area, m ²
t_f	=	time of flight, s
T	=	net thrust, N
\mathbf{u}	=	control vector
u_1, u_2, u_3	=	new control variables
V_x	=	along-track airspeed, m/s
V_z	=	vertical airspeed, m/s
x	=	along-track distance, m
\mathbf{y}	=	state vector
z	=	altitude, m
δ	=	trust-region radius
ϵ	=	tolerance
θ	=	rotor tip-path-plane pitch angle, deg
ρ	=	atmospheric density, kg/m ³

*Assistant Professor, Department of Mechanical, Aerospace, and Biomedical Engineering, Member AIAA, zwang124@utk.edu

†Assistant Professor, Department of Mechanical and Aerospace Engineering, Senior Member AIAA, pwei@gwu.edu

‡Assistant Professor, Department of Mechanical and Aerospace Engineering, Senior Member AIAA, lsun@nmsu.edu

I. Introduction

AVIATION technologies and concepts have reached a level of maturity to enable urban air mobility (UAM) using efficient manned and unmanned aerial vehicles to conduct on-demand and scheduled operations and transport passengers and cargo over short, medium, and long distances at low altitudes [1]. To alleviate the ground transportation congestion, cities are expected to use the third-dimensional space for their mobility needs. Preliminary progress has been made toward defining what future UAM operations would look like, and traditional aviation industry and high-tech newcomers are making huge investments to make the still unproven UAM technology a reality [2]. While initial research has shown the potential of UAM to improve urban transportation efficiency through intelligent use of aerial vehicles, there is a critical need for mathematically rigorous and computationally efficient approaches to better enable future autonomous UAM operations for a wide range of applications, including passenger transport, package delivery, rescue operations, weather monitoring, humanitarian missions, and emergency medical evacuations [3].

Electric vertical takeoff and landing (eVTOL) vehicles with different design approaches are used for most UAM concepts. Compared with the conventional VTOL such as helicopters, the eVTOL vehicles are potentially more efficient, reliable, and flexible due to the improvement enabled by the use of distributed electric propulsion system, which allows more rapid vertical take-off, descent, and landing [4]. In addition, the noise generated by the eVTOL vehicles is significantly less than the helicopters, and the energy consumption and environmental pollution are not big concerns because the electric power is used [5]. Government agencies (e.g., NASA), companies (e.g., Airbus, Joby Aviation, Kitty Hawk, Lilium, Terrafugia, Uber Air, Volocopter, and EHang), and university researchers are developing their eVTOL concepts using different design approaches [6]. In this paper, EHang 184, a multirotor eVTOL vehicle, is selected as a model to study the performance of our proposed trajectory optimization approach.

Tons of publications can be found in the literature on trajectory optimization or path planning for manned and unmanned aerial vehicles with a wide range of applications; however, optimization of cruise, descent, and landing missions in the eVTOL-enabled UAM environment received very little attention. As a representative work in this area, an energy-efficient arrival problem with required time of arrival constraint was considered in [7] for given concepts of operations. A major contribution of this work was the formulation of a fixed-final-time multiphase optimal control problem with energy consumption as the performance index for a multirotor eVTOL vehicle such as EHang 184 [8]. In addition, the authors in [9] developed a similar approach to the optimization of the arrival trajectory for a tandem tilt-wing eVTOL from Airbus A³ [10]. Both problems were solved by GPOPS-II, a general-purpose optimal control solver [11], where the optimal control problem was transformed into a nonlinear programming problem (NLP) using hp-adaptive Gaussian quadrature collocation, and the corresponding NLP was then solved using IPOPT.

In this paper, we address the optimal cruise, descent, and landing problems for eVTOL vehicles via a novel approach. Specifically, the convex optimization is leveraged to enable faster solution processes by exploring the convex structures of the problem. The problem formulation from [7] is considered, and the flight dynamics, boundary conditions, state and control constraints, and objective functional are summarized in Section II. In Section III, the non-convex terms in the problem are convexified, and the solution is sought by solving a sequence of convex optimization problems. Preliminary results are provided in Section IV, and the work is summarized in Section V.

II. Problem Formulation

In this section, the EHang 184 vehicle (see Fig. 1) is used as a model for the study of the trajectory optimization method. However, the formulated problem and the proposed method can be potentially modified and used for other eVTOL vehicles such as CityAirbus and Volocopter 2X, and Airbus Vahana.



Fig. 1 EHang 184 specs and configuration [12].

A. System Dynamics

In this paper, the longitudinal dynamics of the multirotor eVTOL vehicles are decoupled from the lateral dynamics given their symmetrical designs. As a result, only the longitudinal motion is considered, and a two-dimensional (2-D) trajectory generation problem is formulated. The problem formulation used in this paper inherits from [7]. First, the flight dynamics in the longitudinal plane with respect to an inertial reference frame are shown below:

$$\dot{x} = V_x \quad (1)$$

$$\dot{z} = V_z \quad (2)$$

$$\dot{V}_x = \frac{T \sin \theta}{m} - \frac{D_x}{m} \quad (3)$$

$$\dot{V}_z = \frac{T \cos \theta}{m} - \frac{D_z}{m} - g \quad (4)$$

where x and z are the along-track distance and altitude, respectively, which determine the position vector of the vehicle; V_x and V_z are respectively the horizontal and vertical components of the airspeed; T is the net thrust produced by the four arms, and θ is the rotor tip-path-plane pitch angle; m is the mass of the vehicle, and g is the gravitational acceleration. The state and control vectors of the system are defined as:

$$\mathbf{y} = [x, z, V_x, V_z]^T \quad \text{and} \quad \mathbf{u} = [T, \theta]^T \quad (5)$$

respectively, and the horizontal and vertical components of the aerodynamic drag in the fixed inertial frame of reference can be calculated as:

$$D_x = \frac{\rho V_x^2 C_D S_x}{2} \quad \text{and} \quad D_z = \frac{\rho V_z^2 C_D S_z}{2} \quad (6)$$

where ρ is the atmospheric density, C_D is the aerodynamic drag coefficient, and S_x and S_z are the reference front and top flat plate area of the fuselage, respectively. For simplicity, ρ , C_D , S_x , and S_z are assumed to be constant in this paper, and their values are provided in Section IV. As such, D_x and D_z are solely functions of the airspeed components.

B. Flight Constraints

In addition to the system dynamics, there are a number of constraints that the vehicle has to follow to ensure the success of the flight mission. First, the trajectory of the vehicle is assumed to start from an initial condition and terminate at a final state for specific UAM missions. As such, the following boundary conditions are considered:

$$\mathbf{y}(t_0) = \mathbf{y}_0 \quad (7)$$

$$\mathbf{y}(t_f) = \mathbf{y}_f \quad (8)$$

Then, the maximum along-track distance and maximum cruise altitude are defined as follows:

$$0 \leq x \leq x_{\max} \quad (9)$$

$$0 \leq z \leq z_{\max} \quad (10)$$

In addition, the speed of the vehicle should not exceed the maximum value, and a maximum airspeed constraint should be enforced below:

$$\sqrt{V_x^2 + V_z^2} \leq V_{\max} \quad (11)$$

Moreover, the net thrust, T , should be limited within a specific range as shown below:

$$0 \leq T \leq T_{\max} \quad (12)$$

and the vehicle's pitch angle, θ , should also be bounded as follows for the consideration of passenger comfort:

$$|\theta| \leq \theta_{\max} \quad (13)$$

C. Performance Index and Optimal Control Problem

In this paper, the control effort is considered as the performance measure to be minimized, and the objective functional is defined below:

$$J = \int_{t_0}^{t_f} \frac{1}{2} T^2 dt \quad (14)$$

Considering the above objective and constraints, an optimal control problem can be formulated as follows:

Problem 1:

$$\text{Minimize: } \quad (14)$$

\mathbf{y}, \mathbf{u}

$$\text{Subject to: } (1), (2), (3), (4), (7), (8), (9), (10), (11), (12), (13)$$

where our objective is to find the optimal control that minimizes the performance index in (14) while satisfying the dynamics in (1)-(4), the boundary conditions in (7) and (8), the state constraints in (9)-(11), and the control constraints in (12) and (13).

Problem 1 is a constrained, nonlinear optimal control problem that is difficult to solve. One of the promising approaches is to transform the continuous-time problem into a finite-dimensional parameter optimization, which can be solved by nonlinear programming algorithms. The method used in [7] and [9] followed such an approach, and a general-purpose solver was used. However, potential issues may be encountered when nonlinear programming (more specifically, nonconvex optimization) problems are solved. For example, a good initial guess should be carefully selected to enable convergence. Also, the time consumption would be significant when a large number of iterations are required to converge to a solution.

III. A Convex Optimization Approach

In this paper, we address the defined eVTOL trajectory optimization problem (Problem 1) from a novel perspective. Specifically, the convex structure of the problem is explored such that highly efficient convex optimization algorithms can be applied. The primary technical results are provided in this section.

A. Convex Relaxation of Control Constraint

The primary challenge of solving Problem 1 is attributed to the nonlinearity of the system dynamics. As such, the main purpose of our convex approach is to reduce the nonlinear (nonconvex) terms and convert the problem into an equivalent, simpler form. To this end, we first introduce the following new variables:

$$u_1 = T \sin \theta, \quad u_2 = T \cos \theta, \quad \text{and} \quad u_3 = T \quad (15)$$

Then, the equations of motion in (1)-(4) become:

$$\dot{x} = V_x \quad (16)$$

$$\dot{z} = V_z \quad (17)$$

$$\dot{V}_x = \frac{u_1}{m} - \frac{D_x}{m} \quad (18)$$

$$\dot{V}_z = \frac{u_2}{m} - \frac{D_z}{m} - g \quad (19)$$

Along with this transformation, the following constraints should be satisfied:

$$u_1^2 + u_2^2 = u_3^2 \quad (20)$$

and the objective functional in (14) becomes:

$$J = \int_{t_0}^{t_f} \frac{1}{2} u_3^2 dt \quad (21)$$

The conditions in (7)-(11) remain unchanged; however, the control constraints in (12) and (13) can be converted into the following equivalent formulas with respect to the new variables:

$$u_3 \sin(-\theta_{\max}) \leq u_1 \leq u_3 \sin(\theta_{\max}) \quad (22)$$

$$u_3 \cos(\theta_{\max}) \leq u_2 \leq u_3 \cos(0) \quad (23)$$

$$0 \leq u_3 \leq T_{\max} \quad (24)$$

Combining the above equations, a new optimal control problem can be formulated as follows:

Problem 2:

$$\text{Minimize: } \quad (21)$$

\mathbf{y}, \mathbf{u}

$$\text{Subject to: } (16), (17), (18), (19), (7), (8), (9), (10), (11), (20), (22), (23), (24)$$

where the state and control vectors are:

$$\mathbf{y} = [x, z, V_x, V_z]^T \quad \text{and} \quad \mathbf{u} = [u_1, u_2, u_3]^T \quad (25)$$

respectively.

The dynamic equations in (18) and (19) are still nonlinear due to the nonlinear terms of D_x/m and D_z/m ; however, the nonlinearity of the dynamics is reduced because of the introduction of the new control variables in (15). The new objective in (21) takes a convex, quadratic form, and all the constraints in (7)-(11) and (22)-(24) are convex or affine with respect to the state and control variables. However, the new control constraint in (20) represents the surface of a cone, which is nonconvex.

Next, we relax the quadratic equality in (20) into the following inequality form:

$$u_1^2 + u_2^2 \leq u_3^2 \quad (26)$$

Because u_3 is bounded in (24), (24) and (26) together define a convex, solid cone. Then, Problem 2 can be further rewritten into:

Problem 3:

$$\text{Minimize: } \quad (21)$$

\mathbf{y}, \mathbf{u}

$$\text{Subject to: } (16), (17), (18), (19), (7), (8), (9), (10), (11), (26), (22), (23), (24)$$

where the single change from Problem 2 is the replacement of (20) by (26). Problems 1 and 2 are equivalent because Problem 2 is simply a reformulation of Problem 1 by introducing the new control variables and the corresponding constraints. The equivalence between Problems 2 and 3 can be potentially established as well based on the lossless relaxation technique investigated in our previous work [13–15].

B. Convexification of Dynamics and Sequential Convex Programming

At this point, the only nonconvex structure in Problem 3 is the dynamical system defined by (16)-(19). To convexify the dynamics, a pseudo-linear approximation method is utilized. First, we rewrite the dynamic system into the following state-space representation:

$$\dot{\mathbf{y}} = \mathbf{f}(\mathbf{y}) + \mathbf{B}\mathbf{u} \quad (27)$$

where

$$\mathbf{f}(\mathbf{y}) = \begin{bmatrix} V_x \\ V_z \\ -\frac{\rho V_x^2 C_D S_x}{2m} \\ -\frac{\rho V_z^2 C_D S_z}{2m} - g \end{bmatrix} \quad \text{and} \quad \mathbf{B}\mathbf{u} = \begin{bmatrix} 0 \\ 0 \\ \frac{u_1}{m} \\ \frac{u_2}{m} \end{bmatrix}$$

It can be seen that the dynamic system is linear with respect to the controls; however, the state term, $\mathbf{f}(\mathbf{y})$, is nonlinear. A linear approximation method is applied to relax $\mathbf{f}(\mathbf{y})$, and (27) becomes:

$$\dot{\mathbf{y}} \approx \mathbf{f}(\mathbf{y}^*) + \mathbf{A}(\mathbf{y}^*)(\mathbf{y} - \mathbf{y}^*) + \mathbf{B}\mathbf{u} \quad (28)$$

where

$$A(\mathbf{y}^*) = \left. \frac{\partial \mathbf{f}(\mathbf{y})}{\partial \mathbf{y}} \right|_{\mathbf{y}=\mathbf{y}^*} = \begin{bmatrix} 0 & 0 & 1 & 0 \\ 0 & 0 & 0 & 1 \\ 0 & 0 & -\frac{\rho V_x C_D S_x}{m} & 0 \\ 0 & 0 & 0 & -\frac{\rho V_z C_D S_z}{m} \end{bmatrix}_{\mathbf{y}=\mathbf{y}^*}$$

$$B = \begin{bmatrix} 0 & 0 & 0 \\ 0 & 0 & 0 \\ \frac{1}{m} & 0 & 0 \\ 0 & \frac{1}{m} & 0 \end{bmatrix}$$

Equation (28) is linear in both the state and control variables with respect to a reference trajectory, \mathbf{y}^* . To enhance the validity of the linearization, the following trust-region constraint should be included:

$$|\mathbf{y} - \mathbf{y}^*| \leq \delta \quad (29)$$

where δ is the trust-region radius, which is assumed to be fixed in this work. Based the above development, a convexified optimal control problem is obtained as follows:

Problem 4:

$$\text{Minimize: } \quad (21)$$

\mathbf{y}, \mathbf{u}

$$\text{Subject to: } (28), (7), (8), (9), (10), (11), (26), (22), (23), (24), (29)$$

where the objective is convex quadratic, and all the constraints are convex or affine. As such, a globally optimal solution can be achieved, if a solution exists, using convex optimization algorithms such as the interior-point method.

It is worth pointing out that Problem 4 is not equivalent to the previous problems because linearization is applied, and the linearized dynamics are only an approximation to the original dynamics. As such, we cannot obtain a solution to the original problem by solving a single problem defined in Problem 4. However, a successive approach can be developed to gradually converge to a solution to the original problem. The successive solution procedure is summarized as a sequential convex programming (SCP) method shown below:

- 1) Set the iteration number $k = 0$. Provide an initial trajectory $\mathbf{y}^{(0)}$ from the initial state \mathbf{y}_0 to the terminal condition \mathbf{y}_f . In this paper, the line segment that connect the initial and terminal states is chosen as the initial trajectory.
- 2) Set $k = k + 1$. Parameterize Problem 4 using $\mathbf{y}^{(k-1)}$ as the reference trajectory (i.e., \mathbf{y}^*) and solve the resulting convex optimal control problem for a solution $\{\mathbf{y}^{(k)}, \mathbf{u}^{(k)}\}$.
- 3) Check the following convergence condition

$$\sup_{t_0 \leq t \leq t_f} |\mathbf{y}^{(k)} - \mathbf{y}^{(k-1)}| \leq \varepsilon, \quad k > 1 \quad (30)$$

where ε is a prescribed tolerance. If (30) is satisfied, then go to Step 4; otherwise, go back to Step 2 to update and resolve Problem 4.

- 4) The algorithm is converged and a solution is found to be $\{\mathbf{y}^{(k)}, \mathbf{u}^{(k)}\}$.

IV. Numerical Simulations

To investigate the effectiveness of the proposed convex approach, EHang 184 is selected as the simulation model in this paper. The initial and terminal conditions of the mission are defined in Table 1. Other parameters used in the simulations are shown in Table 2. The vehicle is expected to cruise at a constant speed for majority of the flight and then descent and land on the vertipod. The convergence of the proposed SCP method is validated first in YALMIP [16] with the MOSEK solver [17]. Then, GPOPS is used to solve the original problem, and the results are compared to those of the SCP algorithm.

Table 1 Initial and terminal conditions.

Parameter	Value
Initial along-track distance, x_0	0 m
Initial altitude, z_0	500 m
Initial along-track airspeed, V_{x0}	17.78 m/s
Initial vertical airspeed, V_{z0}	0 m/s
Terminal along-track distance, x_f	20,000 m
Terminal altitude, z_f	0 m
Terminal along-track airspeed, V_{xf}	0 m/s
Terminal vertical airspeed, V_{zf}	0 m/s

Table 2 Vehicle parameters for simulations.

Parameter	Value
Vehicle's mass, m	240 kg
Reference front plate area, S_x	2.11 m ²
Reference top plate area, S_z	1.47 m ²
Drag coefficient, C_D	1
Atmospheric density, ρ	1.225 kg/m ³
Gravitational acceleration, g	9.81 m/s ²
Maximum along-track distance, x_{\max}	20,000 m
Maximum altitude, z_{\max}	500 m
Maximum airspeed, V_{\max}	17.78 m/s
Maximum net thrust, T_{\max}	4,800 N
Maximum rotor tip-path-plane pitch angle, θ_{\max}	6 deg
Time of flight, t_f	25 min

A. Convergence of SCP

First, we demonstrate the convergence of our proposed SCP method on the defined UAM mission. Figures 2-5 depict the convergence of the change in the state variables between adjacent iterations. The differences of the states shown in these figures are defined as $|\Delta \mathbf{y}| := \max |\mathbf{y}^{(k)}(t_i) - \mathbf{y}^{(k-1)}(t_i)|$, $i = 1, 2, \dots, N$, where N is the number of the discretized nodes. We can see that these differences converge to the values that satisfy the prescribed tolerance in five iterations. The convergence of the algorithm can also be observed in Fig. 6 where the objective values of all the iterations are presented.

In addition, the profiles of each state variable for all the iterations are shown from dark blue to red in Figs. 7-10. The initial trajectory is simply chosen as the line segment from the initial state to the final condition. We can see that the trajectories converge to the optimal ones (red curves in these figures) from this simple initial guess. The trajectories become very close and the differences are invisible after two iterations. The net thrust produced by the four arms and the rotor tip-path-plane pitch angle are presented in Fig. 11 and 12, respectively, for all the iterations. As can be seen from these figures that the net thrust and the pitch angle fluctuate around constant values for the majority of the flight to minimize the control effort. The converged trajectory leads the vehicle towards the end of the mission to safely land the vehicle on the vertipod while satisfying all the terminal constraints.

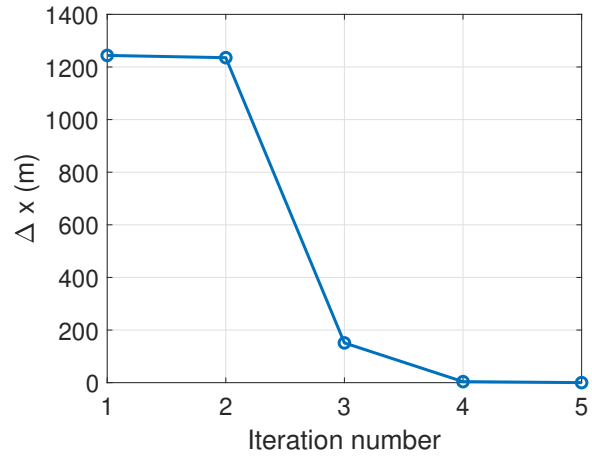


Fig. 2 Convergence of Δx between consecutive iterations.

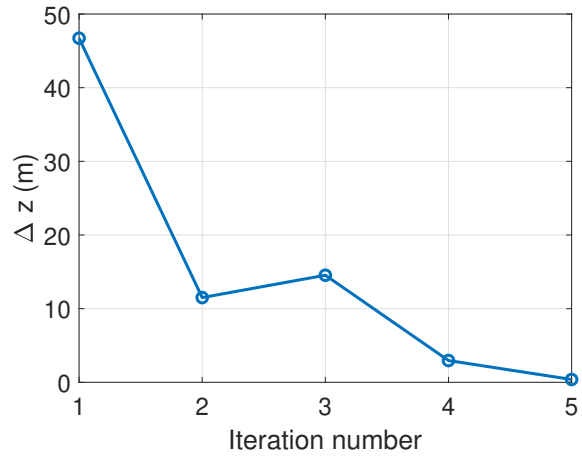


Fig. 3 Convergence of Δz between consecutive iterations.

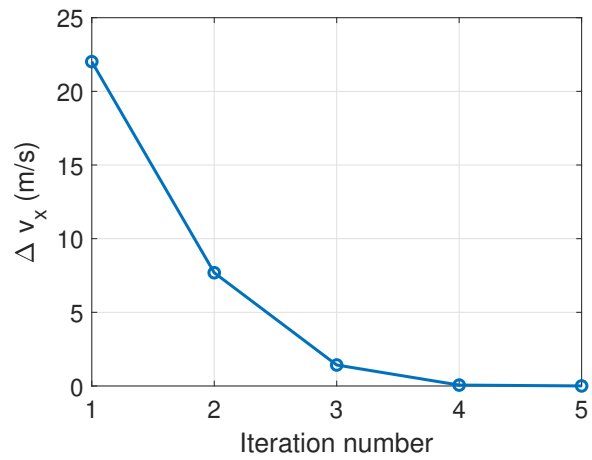


Fig. 4 Convergence of ΔV_x between consecutive iterations.

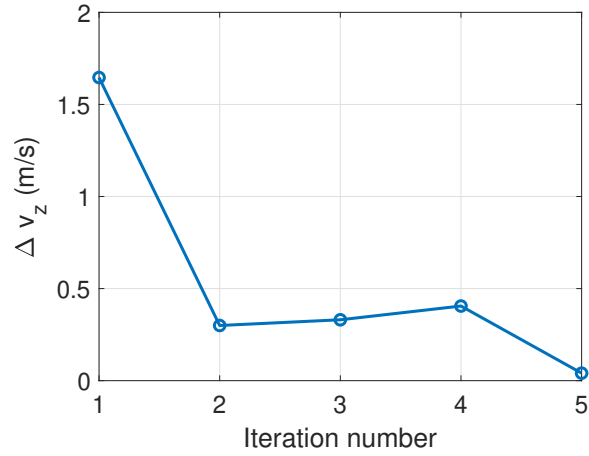


Fig. 5 Convergence of ΔV_z between consecutive iterations.

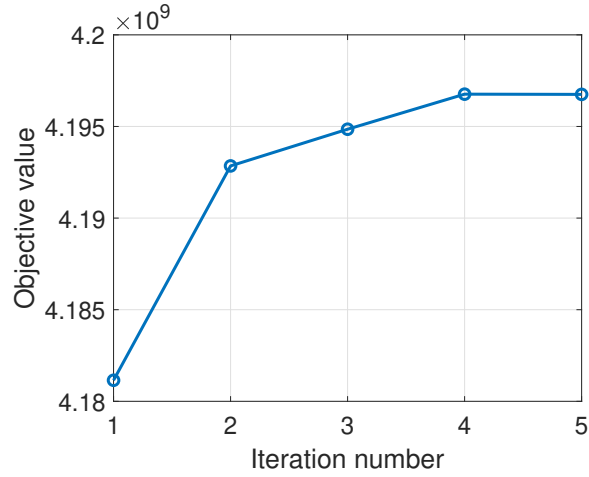


Fig. 6 Convergence of the objective values.

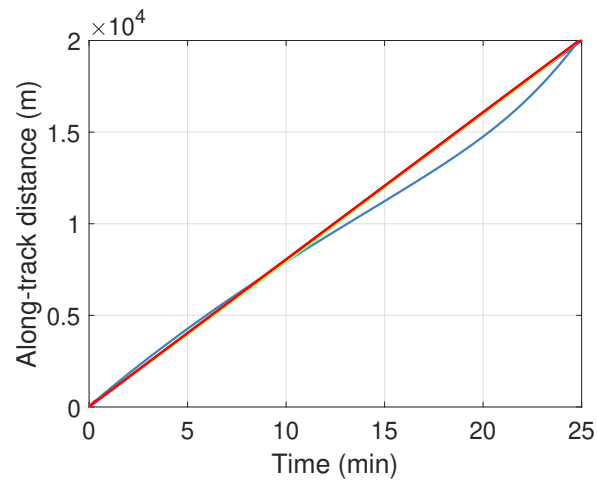


Fig. 7 Convergence of the along-track distance (x) profiles.

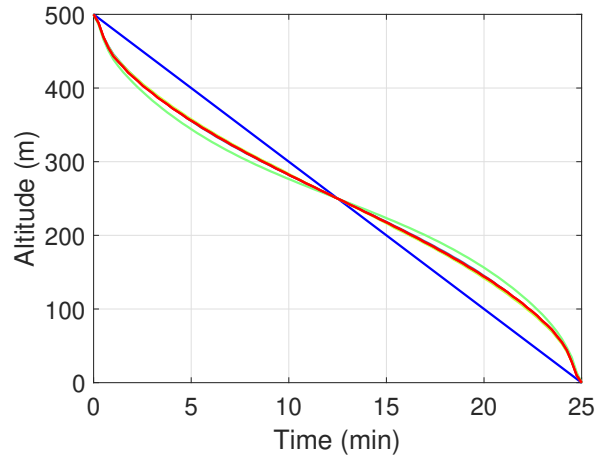


Fig. 8 Convergence of the altitude (z) profiles.

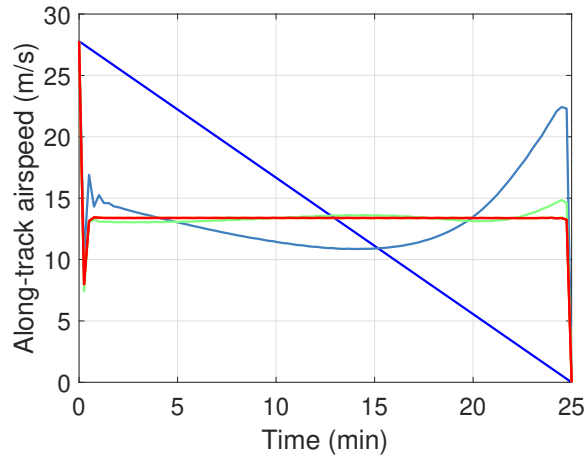


Fig. 9 Convergence of the along-track airspeed (V_x) profiles.

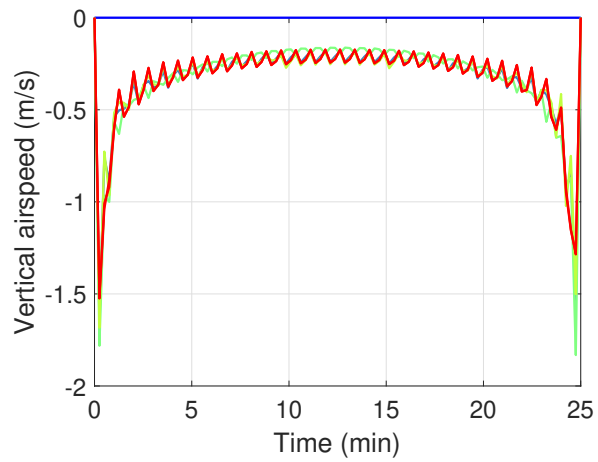


Fig. 10 Convergence of the vertical airspeed (V_z) profiles.

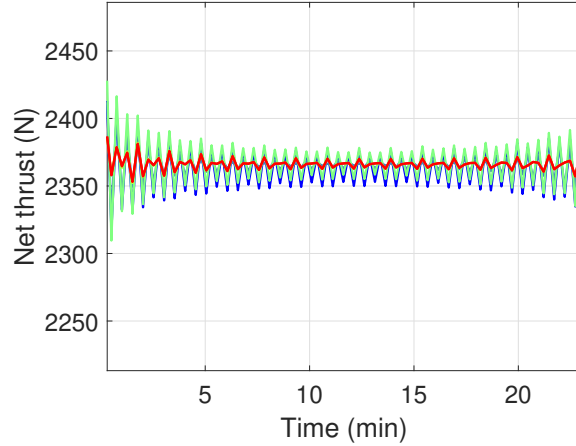


Fig. 11 Convergence of the along-track control component ($u_1 = T \sin \theta$) profiles.

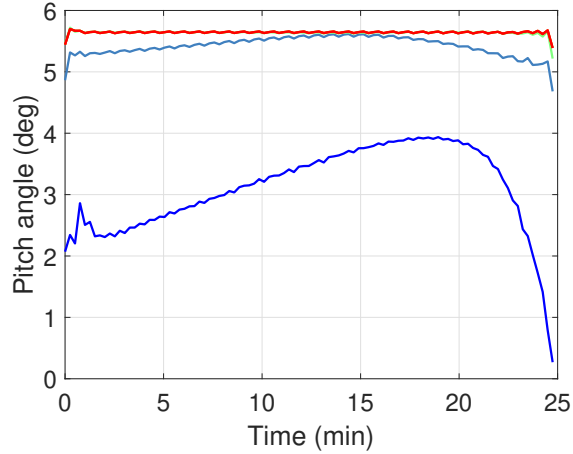


Fig. 12 Convergence of the rotor tip-path-plane pitch angle (θ) profiles.

B. Compare to GPOPS

In addition to the convergence of the proposed convex approach, we also investigate the accuracy and optimality of the converged solution through comparison with other solvers. In this paper, a powerful optimal control package, GPOPS, is used to solve the original nonconvex optimal control problem (Problem 1). The results are compared with those from the SCP in Figs. 13-18. We can see that the profiles obtained from the SCP and GPOPS are very close, and the profiles of each state and control variable behave the similar trend. For example, the vehicle cruises at a constant along-track airspeed (13.4 m/s) and the vertical airspeed remains close to zero for the majority of the mission to minimize the control cost. Also, the net thrust changes around 2,365 N and the optimal pitch angle fluctuates around 5.6 deg to maintain the steady cruise flight. Obvious changes in the motion during the last minute can be observed for safe and accurate descent and landing. As such, the preliminary results show that these two solvers converge to similar optimal solutions for the simulation case considered in this paper. In addition, the curves obtained from the developed SCP method are much smoother than those from GPOPS where high-frequency jitters are present in the figures. Based on these preliminary results, we will explore more efficient algorithms [18–21] to improve the performance and robustness of our proposed method in the future.

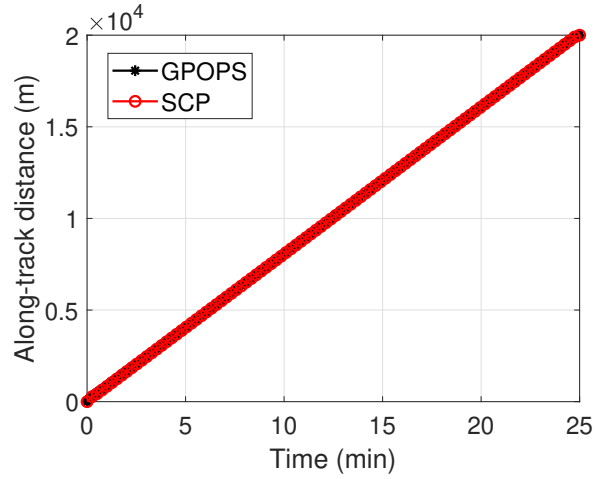


Fig. 13 Comparison of the along-track distance (x) profiles.

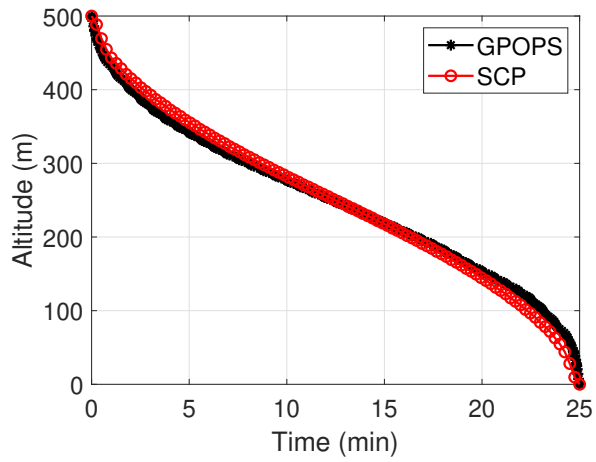


Fig. 14 Comparison of the altitude (z) profiles.

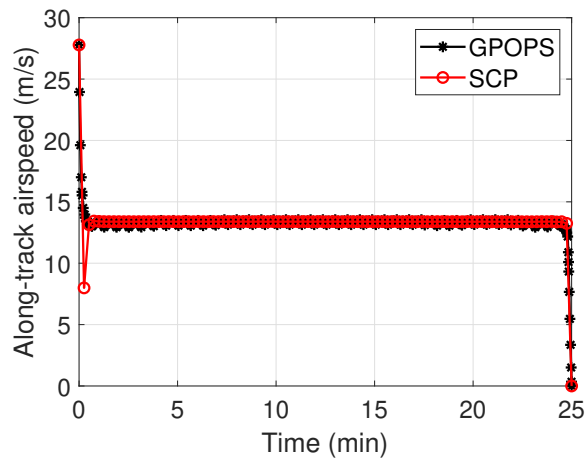


Fig. 15 Comparison of the along-track airspeed (V_x) profiles.

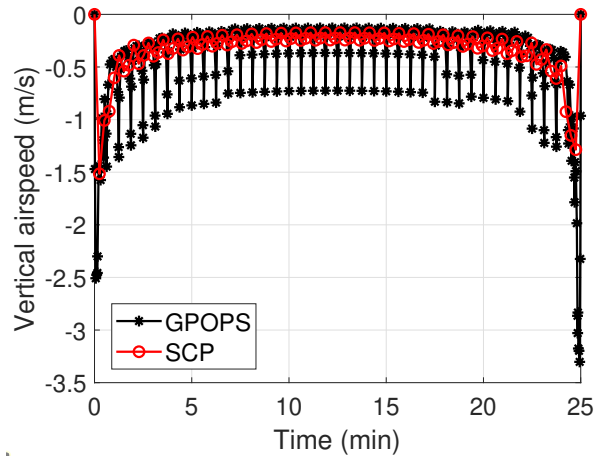


Fig. 16 Comparison of the vertical airspeed (V_z) profiles.

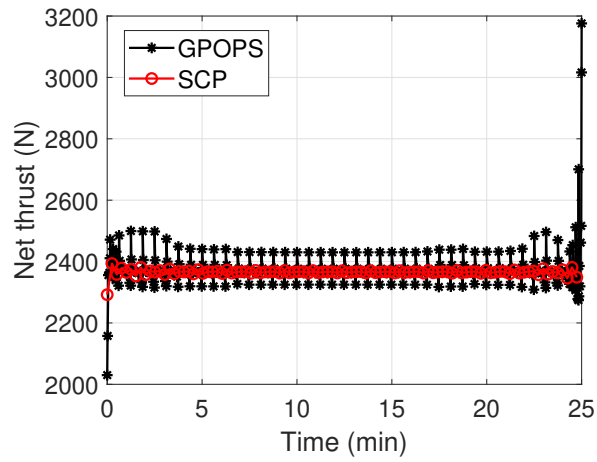


Fig. 17 Comparison of the net thrust (T) profiles.

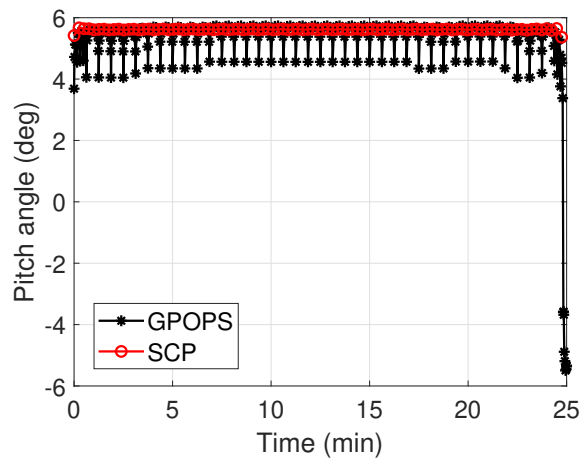


Fig. 18 Comparison of the rotor tip-path-plane pitch angle (θ) profiles.

V. Conclusion

UAM has received a lot of attention in recent years as a promising means to alleviate the ground traffic and improve the urban transportation. eVTOL vehicles have shown great potential to achieve these purposes. In this work, we focus on the optimal design of cruise, descent, and landing trajectories for UAM missions, and the problem is addressed from a novel, convex-optimization-based approach. To this end, we first formulate the trajectory optimization problem as a multi-constrained, nonconvex optimal control problem. Then, the nonlinearity of the dynamics is reduced by introducing several new control variables. A convexification technique is utilized to reduce the nonconvex control constraint into a convex, solid cone. Through successive linear approximations, a convex optimal control problem is obtained. Finally, a sequential convex programming approach is developed, where the solution from the previous iteration is used to parameterize and solve the convex optimal control problem in the current iteration until the process is converged. A simulation case is used to demonstrate the proposed approach, and preliminary results have shown the convergence of accuracy of the developed algorithm.

References

- [1] Uber-Elevate, “Fast-Forwarding to the Future of On-Demand, Urban Air Transportation,” <https://www.uber.com/elevate.pdf>, 2016.
- [2] Thippavong, D. P., Apaza, R., Barmore, B., Battiste, V., Burian, B., Dao, Q., Feary, M., Go, S., Goodrich, K. H., Homola, J., Idris, H. R., Kopardekar, J. B., P H Lachter, Neogi, N. A., Ng, H. K., Oseguera-Lohr, R. M., Patterson, M. D., and Verma, S. A., “Urban Air Mobility Airspace Integration Concepts and Considerations,” *2018 Aviation Technology, Integration, and Operations Conference*, Atlanta, Georgia, USA, 2018.
- [3] Porsche-Consulting, “The Future of Vertical Mobility,” <https://fedotov.co/wp-content/uploads/2018/03/Future-of-Vertical-Mobility.pdf>, 2018.
- [4] Kim, H. D., Perry, A. T., and Ansell, P. J., “A Review of Distributed Electric Propulsion Concepts for Air Vehicle Technology,” *2018 AIAA/IEEE Electric Aircraft Technologies Symposium (EATS)*, Cincinnati, OH, USA, 2018.
- [5] Prevot, T., Rios, J., Kopardekar, P., Robinson III, J. E., Johnson, M., and Jung, J., “UAS Traffic Management (UTM) Concept of Operations to Safely Enable Low Altitude Flight Operations,” *16th AIAA Aviation Technology, Integration, and Operations Conference*, Washington, D.C., USA, 2016.
- [6] “The Global Urban Air Mobility Project Report,” <https://www.urbanairmobilitynews.com/wp-content/uploads/2019/03/Global-Urban-Air-Mobility-Report-7-March-2019.pdf>, 2019.
- [7] Pradeep, P., and Wei, P., “Energy-Efficient Arrival with RTA Constraint for Multicopter eVTOL in Urban Air Mobility,” *Journal of Aerospace Information Systems*, Vol. 16, No. 7, 2019, pp. 263–277.
- [8] EHang-184, “EHang 184 Autonomous Aerial Vehicle (AAV),” <https://www.aerospace-technology.com/projects/ehang-184-autonomous-aerial-vehicle-aav/>, 2018.
- [9] Pradeep, P., and Wei, P., “Energy Optimal Speed Profile for Arrival of Tandem Tilt-Wing eVTOL Aircraft with RTA Constraint,” *IEEE CSAA Guidance, Navigation and Control Conference (GNCC)*, Fujian, China, 2018.
- [10] Lovering, Z., “Vahana Configuration Trade Study Part I,” <https://acubed.airbus.com/blog/vahana/vahana-configuration-trade-study-part-i/>, 2016.
- [11] Patterson, M. A., and Rao, A. V., “GPOPS-II: A MATLAB Software for Solving Multiple-Phase Optimal Control Problems Using hp-Adaptive Gaussian Quadrature Collocation Methods and Sparse Nonlinear Programming,” *ACM Transactions on Mathematical Software (TOMS)*, Vol. 41, No. 1, 2014, pp. 1–37.
- [12] Bacchini, A., and Cestino, E., “Electric VTOL Configurations Comparison,” *Aerospace*, Vol. 6, No. 3, 2019, p. 26.
- [13] Wang, Z., and Grant, M. J., “Minimum-Fuel Low-Thrust Transfers for Spacecraft: A Convex Approach,” *IEEE Transactions on Aerospace and Electronic Systems*, Vol. 54, No. 5, 2018, pp. 2274–2290.
- [14] Wang, Z., and Grant, M. J., “Optimization of Minimum-Time Low-Thrust Transfers Using Convex Programming,” *Journal of Spacecraft and Rockets*, Vol. 55, No. 3, 2018, pp. 586–598.
- [15] Wang, Z., and McDonald, S. T., “Convex Relaxation for Optimal Rendezvous of Unmanned Aerial and Ground Vehicles,” *Aerospace Science and Technology*, Vol. 99, 2020.

- [16] Löfberg, J., “YALMIP : A Toolbox for Modeling and Optimization in MATLAB,” *In Proceedings of the CACSD Conference*, Taipei, Taiwan, 2004.
- [17] “MOSEK Optimization Toolbox for MATLAB,” *User’s Guide and Reference Manual*, 2019.
- [18] Wang, Z., and Lu, Y., “Improved Sequential Convex Programming Algorithms for Entry Trajectory Optimization,” *Journal of Spacecraft and Rockets*, Vol. 57, No. 6, 2020, pp. 1373–1386.
- [19] Wang, Z., and McDonald, S. T., “Optimal Rendezvous of Unmanned Aerial and Ground Vehicles via Sequential Convex Programming,” *AIAA Aviation Forum*, Dallas, Texas, 2019.
- [20] McDonald, S. T., and Wang, Z., “Real-Time Optimal Trajectory Generation for UAV to Rendezvous with an Aerial Orbit,” *AIAA Aviation Forum*, Dallas, Texas, 2019.
- [21] Sun, L., Hedengren, J. D., and Beard, R. W., “Optimal Trajectory Generation using Model Predictive Control for Aerially Towed Cable Systems,” *Journal of Guidance, Control, and Dynamics*, Vol. 37, No. 2, 2014, pp. 525–539.